

Faraday Discussions

Accepted Manuscript



This is an Accepted Manuscript, which has been through the Royal Society of Chemistry peer review process and has been accepted for publication.

Accepted Manuscripts are published online shortly after acceptance, before technical editing, formatting and proof reading. Using this free service, authors can make their results available to the community, in citable form, before we publish the edited article. We will replace this Accepted Manuscript with the edited and formatted Advance Article as soon as it is available.

You can find more information about Accepted Manuscripts in the [Information for Authors](#).

Please note that technical editing may introduce minor changes to the text and/or graphics, which may alter content. The journal's standard [Terms & Conditions](#) and the [Ethical guidelines](#) still apply. In no event shall the Royal Society of Chemistry be held responsible for any errors or omissions in this Accepted Manuscript or any consequences arising from the use of any information it contains.

This article can be cited before page numbers have been issued, to do this please use: T. Roberts, M. Cesler-Maloney and W. Simpson, *Faraday Discuss.*, 2024, DOI: 10.1039/D4FD00177J.

ARTICLE

Low-cost electrochemical gas sensing of vertical differences in wintertime air composition (CO, NO, NO₂, O₃) in Fairbanks, Alaska

Tjarda J. Roberts,^{*a,b} Meeta Cesler-Maloney^c and William Simpson^c

Received 00th January 20xx,

Accepted 00th January 20xx

DOI: 10.1039/x0xx00000x

Wintertime Fairbanks, Alaska, experiences episodes of severely poor air quality, when local emissions (e.g. from home-heating, vehicular) are enhanced by cold conditions and are trapped by temperature inversions. Monitoring of atmospheric composition, and in particular vertical gradients in composition, is challenging under cold Arctic conditions. This study demonstrates that multiple sets of low-cost electrochemical sensors can provide accurate measurement of CO, NO, NO₂, O₃ air composition across wide-ranging cold Arctic temperatures (0°C to -30 °C). The sensors quantify vertical gradients in downtown Fairbanks atmospheric composition during winter 2021. Low-cost electrochemical sensors (with co-measured temperature) were characterised by cross-comparison to a regulatory air quality monitoring site. We demonstrate excellent agreement of the electrochemical sensors with the reference monitors ($R^2 > 0.77-0.98$), with mean absolute errors <5 ppbv (NO, NO₂, O₃) and <50 ppbv (CO) over gas-ranges of 10's-100's, and 3000 ppbv, respectively, sufficient for the low-cost electrochemical sensors to quantitatively investigate NO-NO₂-O₃ atmospheric chemistry. During four weeks in February-March 2021, sensors placed on the rooftop (20m) and base (3m) of a building in downtown Fairbanks identify strong gradients in atmospheric composition over a very short <20 m vertical scale at times when near-surface temperature inversions were present. At night, CO and NO_x were more concentrated at the surface than aloft, and surface ozone was depleted whilst sometimes being present aloft. During daytime, when solar radiation heated the surface, inversions were disrupted by efficient vertical mixing that mixed in ozone-rich air from above. The low-cost sensor observations demonstrate near-surface pollutant trapping was correlated to thermal inversions, trace O₃-NO_x atmospheric chemistry, and quantify a local O_x source from direct "primary" NO₂ emissions, with a directly emitted NO₂:NO_x ratio of 0.13 mol/mol. The sensors also characterise NO_x emissions finding a NO_x:CO of 0.18 mol/mol. When well-characterised, low-cost electrochemical sensors can provide valuable measurements of local emissions and vertically-resolved atmospheric composition, with sufficient accuracy to trace atmospheric chemistry in cold and stable wintertime urban environments.

Introduction

Observations of atmospheric composition in the Arctic are sparse yet particularly relevant in the urban Arctic due to local emissions^[1]. Cities such as Fairbanks, Alaska, can experience severe air pollution episodes during winter, when enhanced local emissions, e.g. from traffic and home-heating^[2,3], become trapped near to the surface by temperature inversions^[4-7]. Similar processes can also occur at lower latitude basin and valley sites leading to episodes of severe wintertime air quality in locations such as in Salt Lake Valley, Utah^[8] and Grenoble, France^[9]. A stable temperature gradient inhibits mixing in the vertical, whilst sheltering by surrounding topography protects from mixing in the horizontal, leading to the development of persistent cold-air pools and the accumulation of surface air

pollution^[10]. The atmosphere above Fairbanks contains multiple thermal inversion layers during winter^[11,12]; elevated inversion layers can occur up to several hundreds to thousands meters aloft. Recent evidence highlights that very shallow inversions that develop at the surface or within tens of meters of the surface exert an important role on downtown Fairbanks air quality through trapping of surface emissions; Cesler-Maloney et al.^[13] report vertical differences in particulate matter and ozone between the surface and 20 m aloft during surface-based inversions on similar vertical spatial scales, also supported by vehicle-based particle mapping^[14]. These findings focus our attention on the atmosphere in the tens of meters above Fairbanks in which gradients in atmospheric composition can be unusually strong compared to lower latitudes. To better understand the causes of extreme enhanced surface pollution during Fairbanks wintertime, and associated chemistry and mixing processes affecting wintertime atmospheric composition, it is necessary to measure at such levels aloft as well as at the surface. However, many traditional instruments that quantify atmospheric composition are too demanding in their power consumption, weight or maintenance needs for this purpose. Furthermore, the Arctic presents a particular challenge to such instrumentation due to the very cold

^a LMD/IPSL, ENS, Université PSL, Ecole Polytechnique, Institut Polytechnique de Paris, Sorbonne Université, CNRS, Paris, France. Tjarda.Roberts@lmd.ipsl.fr

^b LPC2E, OSUC, Université d'Orléans, CNRS, CNES, 45071, Orléans, France.

^c Geophysical Institute and Department of Chemistry and Biochemistry, University of Alaska Fairbanks, AK 99775

Supplementary Information available: One Sup. Mat. file submitted. See DOI: 10.1039/x0xx00000x



temperatures that can reach as low as $-40\text{ }^{\circ}\text{C}$ during Fairbanks winter. This motivates our field-demonstration of low cost, highly portable and low power electrochemical gas sensors to continuously measure CO, NO, NO₂ and O₃ wintertime gas composition in the atmosphere above Fairbanks, Alaska.

Low-cost electrochemical sensing of air pollution and their potential for investigations of Arctic atmospheric composition.

Over the last decade, networks of miniature electrochemical (amperometric) sensors have been applied to monitor surface air quality in low-latitude locations, e.g.^[15-27]. These studies mostly apply low-cost electrochemical sensors for horizontal spatial mapping of surface air quality, or air pollutant exposure. Advantages of these sensors over traditional atmospheric instrumentation include their low power requirement and low cost (0.01 Watts and about hundred euros per sensor). One small instrument (hundreds g up to a few kg) can house multiple electrochemical sensors alongside other small gas and particle sensors and data-acquisition electronics. Commercial sensor packages (at a cost of several thousand euros) typically do not require specialist installation, and can deliver fully autonomous monitoring of multiple pollutant gases over many months with quasi real-time transfer of the measurements to a data-cloud. These advantages facilitate the deployment of multi-sensor monitoring networks, applications on mobile platforms, e.g.¹⁵, or in remote locations, e.g.^{25,27}. However, sensor accuracy, biases and drift can be significant limitations e.g.^{23,24}, and are the main disadvantages of low-cost electrochemical sensors compared to traditional instruments. These limitations tend to become critical at low gas abundances thus are particularly pertinent in research investigations of atmospheric chemistry where ozone varies by just tens of ppbv. Indeed, few studies have exploited low-cost electrochemical sensors to investigate atmospheric chemistry, which requires robust ppbv-level detection of gases such as NO, NO₂, and O₃. A consistent sensor performance with ppbv-level accuracy is also required to quantify vertical differences in atmospheric composition over time. Here we deploy two sets of well-calibrated sensors to demonstrate low-cost electrochemical sensing of atmospheric composition at the ppbv-level over weeks to months in the urban Arctic atmosphere. We thereby trace O₃-NO-NO₂ atmospheric chemistry and quantify vertical differences in wintertime CO, NO, NO₂ and O₃ composition of the atmosphere over very short vertical scales (3 m to 20 m) above Fairbanks, Alaska.

Vertically-resolved measurements of atmospheric gas composition are needed during surface pollution episodes. In Arctic cities such as Fairbanks (and some lower-latitude urban environments), the occurrence and severity of wintertime surface pollution episodes depends crucially on the degree and scale of the vertical mixing. Episodes of poor air quality are more severe when local emissions become trapped and accumulate near to the surface, and less severe when the emissions can disperse and dilute in the vertical. As recently highlighted^[13,14], near-surface thermal inversions exert a critical role on the trapping of locally-emitted pollutants very close to

the surface, leading to severe air quality episodes in Fairbanks. Under calm winds, such inversions can develop during the cold Arctic night, but can be disrupted by daytime solar heating of the surface during Fairbanks late-winter (February to March), to cause enhanced vertical mixing and dilution of the surface pollution. Atmospheric chemistry furthermore influences the composition of the wintertime atmosphere. For example, reaction cycles involving ozone control the partitioning between NO and NO₂ in NO_x, and can convert NO_x into nitrate particulate matter through photolytic oxidation and non-photolytic mechanisms (the latter may have particular relevance in Fairbanks dimly-lit winter^[13]). Such chemical reactions progress as a function of the concentrations of pollutants and oxidants, e.g. ozone, and depend on the composition of the local emissions and also on how vertical mixing distributes pollutants and may promote chemical reactions through in-mixing of cleaner and more ozone-rich air masses from aloft. This study investigates the vertical distribution in atmospheric composition above Fairbanks, Alaska. We demonstrate continuous monitoring of atmospheric CO, NO, NO₂ and O₃ abundances by low-cost electrochemical sensors at two heights (at 3m and 20m by sensor rooftop deployment) during a four-week period in February-March 2021. We correlate these measurements to inversions traced by temperature sensors on a 11m mast. We quantify vertical gradients in atmospheric composition across the diurnal cycle. We relate the sensor observations to trapping of locally emitted pollutants by nighttime inversions, enhanced vertical mixing during daytime, and to atmospheric chemistry. Using low-cost electrochemical sensors we also characterize local Fairbanks emissions with a focus on CO, NO_x, and O_x (signifying primary NO₂) emissions.

Methods

Low-cost electrochemical sensing of CO, NO, NO₂ and Ozone.

Two sets of four miniature electrochemical gas sensors (CO-A4, NO-A4, NO₂-A43F, O_x-A431, Alphasense Sensor Technology Company) were used to measure CO, NO, NO₂ and O₃ at 0.1 Hz with data hourly-averaged for the purpose of this study. The cm-sized electrochemical sensors were housed with downward facing diffusion face exposed directly to the air within two identical mains-powered instruments (EMSOL Praxis Unit, originally by SouthCoastScience), that co-measured the sensor temperature (Sensirion SHT3x), and transferred sensor signals to a data cloud by 4G cellular phone modem in near real-time. For each target gas, the raw electrochemical sensor signal, (S , working electrode current, recorded as voltage via 0.8 mV/nA gain of the Alphasense AFE electronics) was analysed to extract mixing ratios [X , ppbv], by rearranging the sensor equation, e.g.^[28], $S = B + s_x \cdot [X]$, where the baseline (B , Volts) and sensor sensitivity (s , Volts/ppbv) are sensor-specific and temperature dependant, and were calibrated by cross-comparison to air-quality monitoring data. As the O_x-A431 sensor is sensitive to both ozone and NO₂, the measurement of ozone required subtraction of the interference of NO₂ (cross-sensitivity c_{SNO_2} multiplied by NO₂ mixing ratio i.e. $c_{\text{SNO}_2} \cdot [\text{NO}_2]$) from the O_x-A431 sensor signal, S_{O_3} , (see Alphasense.com and^[29]). The other



sensors exhibited negligible inter-gas cross-sensitivities. The cross-comparison calibrations to air quality reference monitors were undertaken at the NCORE site during two periods, from January 7th to February 7th 2021, and from 9th March to 31st March 2021. The NCORE site is an air-quality monitoring site located in downtown Fairbanks operated by the ADEC (Alaska Department of Environmental Conservation). A range of reference monitors for gases and particulate matter are operated within heated trailers at NCORE, delivering air quality datasets that are publicly available from the DEC website and contribute to the US Environmental Protection Agency monitoring network. The NCORE gas monitoring system was upgraded in 2020. This study uses NCORE datasets from the CO analyser (Teledyne API T300U), NO and NO_y analyser (Teledyne T200U) and ozone analyser (Thermo 49iQ), supplied as hourly averages alongside ambient temperature. NO₂ was not directly measured by DEC at NCORE in 2021. An indirect DEC measurement of NO₂ is approximated by NO₂ = NO_y-NO. This approximation is appropriate for the polluted conditions of downtown Fairbanks, as demonstrated by intercomparison of NO_x and NO_y instruments deployed by DEC at NCORE during previous winters (Supplementary Material Figure S1). During January-March 2021 the DEC ozone analyser at NCORE experienced some issues in drifting baseline stability, leading to data gaps and uncertainty in the reported values. We address this uncertainty by comparing the provisional NCORE ozone data provided by DEC to another ozone monitor (Dasibi 1008-RS O₃ photometric analyzer) that was deployed in a heated trailer at the nearby CTC site (~500 m distance) during February 2021 to deliver a corrected surface ozone measurement (Supplementary material, Figure S2).

Field-campaign: atmospheric composition measured at two heights (3m and 20m) in downtown Fairbanks

To probe vertical differences in Fairbanks air composition, the sensors were deployed at two heights at the CTC site from 7th February to 9th March 2021. The CTC site is located about 500 m south from the NCORE site, in downtown Fairbanks. At 20m high, the CTC (University of Alaska Community Technical College) is one of the tallest buildings in Fairbanks. One set of sensors (Praxis 430) was deployed on the CTC roof at about 20 m above ground, the other (Praxis 429) was deployed on top of a trailer at the CTC base, approximately 3m above ground. These two-height gas measurements of CO, NO, NO₂, and O₃ were complemented by measurements of the inversion strength over the 4-week period. Ambient temperature at 11m and 3m height was measured on a mast near to the CTC building (with aspirated thermocouples^[13]), enabling to derive the 11-3m temperature difference. Ambient temperature was not measured at 20m on the CTC roof, but the temperature of the electrochemical sensors was monitored, from which a 20-3m T_{sens} sensor temperature difference can be derived.

Results and discussion

Low-cost electrochemical sensing of atmospheric composition (CO, NO, NO₂ and O₃) in downtown Fairbanks

Time-series from the two sets of four low-cost electrochemical sensors for CO, NO, NO₂ and O₃ that were deployed in downtown Fairbanks, at the NCORE site (3 m) for the cross-calibration to air quality analysers (shaded region, 7 Jan – 7 February and 9 March - 31 March, 2021), and at the nearby-located CTC site (3m) and CTC building roof (20m) for measuring vertical gradients (unshaded region, 7 February – 9 March 2021) are shown in Figure 1a. Sensors were deployed continuously, with hourly averages presented in this study. Figure 1a demonstrates that the sensors exhibited negligible drift over the three month period. An estimate of sensor accuracy is given in Table 1, that presents analysed sensor output compared to air quality analysers in terms of R², RMSE Root Mean Square Deviation, and Mean absolute error, where alternate hourly data has been used in the cross-calibrations and statistical analyses (n > 500 data points for each, across the total cross-comparison period). From this evaluation, mean absolute errors are < 50 ppbv (CO) and < 5 ppbv (NO, NO₂, O₃). This lends confidence to the field-campaign measurements at the CTC site (unshaded region, 7 February – 9 March 2021) when significant differences in measured air composition can be seen between the 20m rooftop and 3m surface air during surface pollution events. During January to March, Fairbanks typically experiences the transition from being dimly-lit with severe surface air pollution to a very strong diurnal solar cycle, and less severe and more variable surface air pollution conditions. Ambient temperature generally warms during these months, but with substantial temporal variability (ranging from below -30 °C to above 0 °C during January-March 2021). Furthermore, from February onwards, and depending on local meteorological conditions, surface heating by solar radiation can cause strong diurnal temperature changes, that sometimes exceed 10 °C, as was observed during the Fairbanks winter of 2021, Figure 1a. Near-surface wind-speeds were low (averaging around 0.5 m/s, data not shown), confirming calm conditions suitable for the development of thermal inversions. During the CTC field-campaign (7 February – 9 March 2021), the low-cost sensors measurements show that pollution was more enhanced at the surface (3m) than aloft (20m), particularly during the periods with ambient temperature minima. Such strong vertical gradients in atmospheric composition indicate near-surface trapping of local pollutants by thermal inversions at night.

View Article Online
DOI: 10.1039/D4FD00177J



Table 1. Statistics of the two electrochemical sensor sets (Praxis P430 and Praxis 429) compared to ADEC Air-quality Monitors when co-located at NCORE EPA monitoring site in downtown Fairbanks (7 Jan – 7 February and 9 March - 31 March, 2021, shaded regions Figure 1a), across sensor temperatures $-30^{\circ}\text{C} \geq T_{\text{sens}} \leq 0^{\circ}\text{C}$. RMSE: Root Mean Square Deviation. MAE: Mean Absolute Error. Analysis and calibration are performed on alternate data points ($n > 500$ each) during this cross-comparison period to enable statistics on the sensor gas measurement independent from the data used for sensor calibration.

View Article Online
DOI: 10.1039/D4FD00177J

Sensor Set	Sensor Type	Target Gas	Max ppbv	R ²	RMSE ppbv	MAE ppbv
P430	CO-A4	CO	2243	0.96	70	45
	NO-A4	NO	327	0.98	6.9	4.2
	NO2-A43F	NO ₂	51	0.88	3.5	2.6
	Ox-A431	O ₃	27	0.90	3.0	2.0
P429	CO-A4	CO	2001	0.95	69	47
	NO-A4	NO	252	0.98	7.2	4.6
	NO2-A43F	NO ₂	44	0.86	3.5	2.6
	Ox-A431	O ₃	27	0.94	2.1	1.4



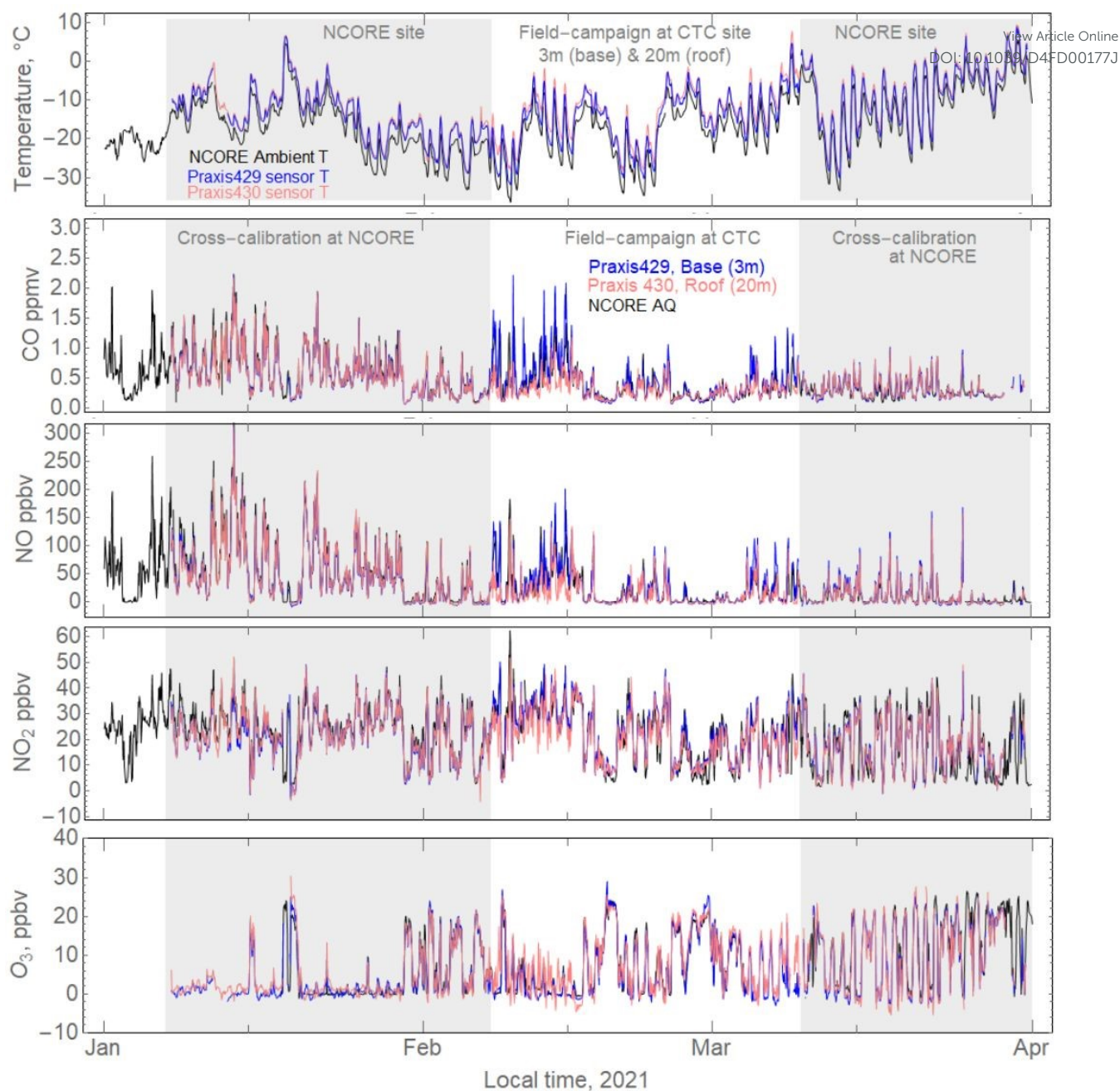


Figure 1a. Time-series of hourly CO, NO, NO₂, O₃ gas abundances measured by low-cost electrochemical sensor in two instruments (Praxis 430, pink and Praxis 429, blue) in downtown Fairbanks. Also shown are measurements by DEC air quality monitors at the Fairbanks NCORE EPA monitoring site. During January 9-February 7 and March 9-March 31 the sensors were co-located at NCORE (3m, shaded regions), as part of cross-calibration. During February 7 – March 9 the sensors were located at CTC site (500m south of NCORE) at the base (3m height, Praxis429, blue) and CTC building rooftop (20m height, Praxis 430, pink), and show distinct differences in air composition. Also shown is ambient temperature monitored at NCORE (3m) and sensor temperatures that are slightly (~5 °C) above ambient.



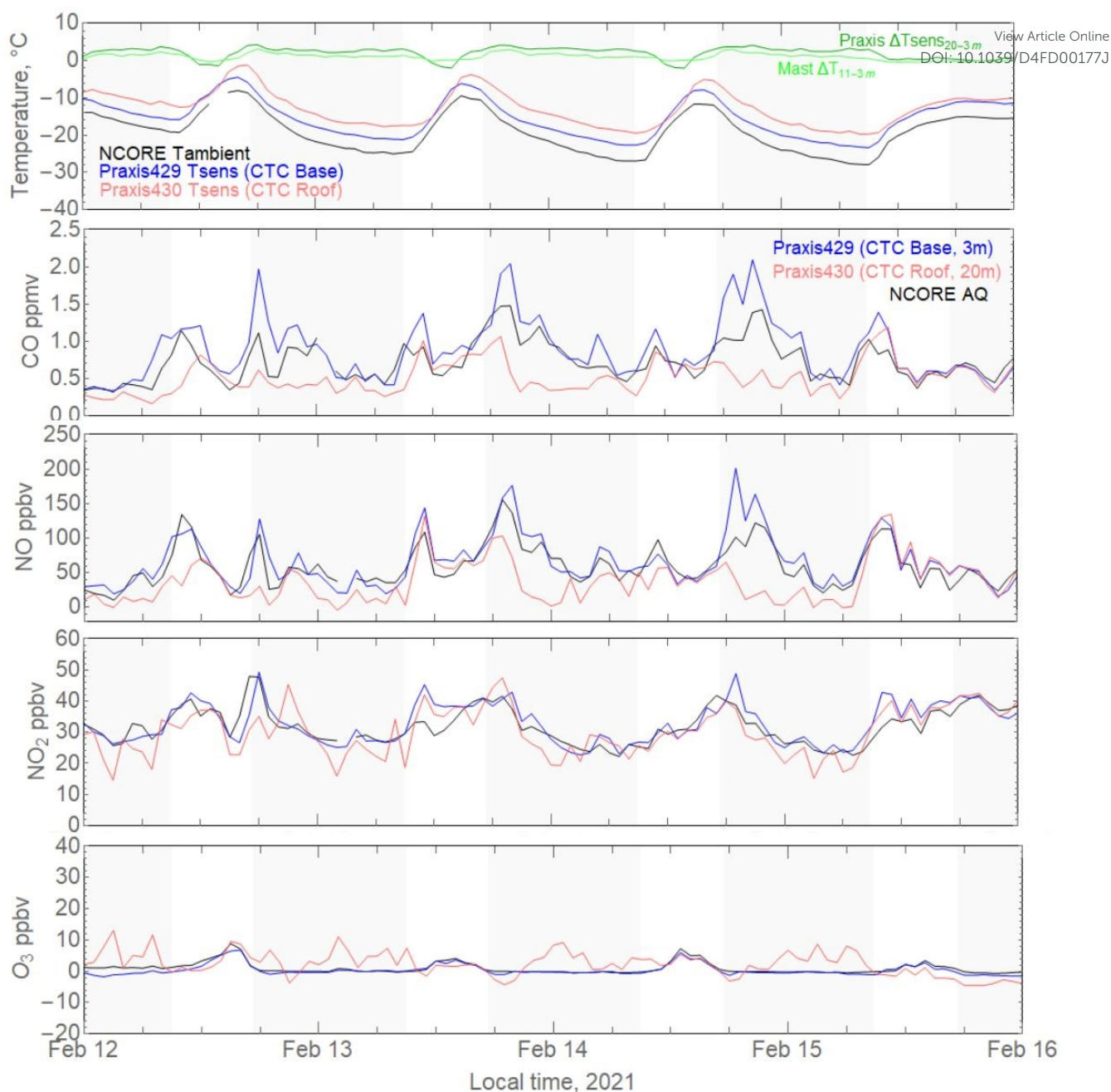


Figure 1b. Hourly CO, NO, NO₂, O₃ measured by two sets of low-cost electrochemical sensors at two heights: CTC base at 3m (Praxis 429, blue) and on the CTC building roof at 20m (Praxis 430, pink). Also shown is surface (3m) air quality monitoring data from the nearby NCORE site. Shaded/unshaded denotes night/day. Data is as in Figure 1a, here with a zoom on the February 12 to February 16 period that exhibits the strongest night-time trapping of pollutants as observed by the two-height measurements. Ozone exhibits an inverse trend with cleaner air aloft during night. Also shown are ambient temperature at NCORE, and sensor temperature of the two Praxis. In addition, the first panel shows vertical differences in the measured temperature of the low-cost sensors (20m -3m) and of ambient temperature measured by thermocouples on a nearby mast (11m-3m) that denote presence of night-time inversions.



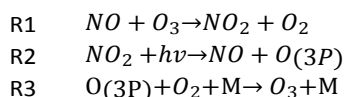
Strong vertical gradients in atmospheric composition in 20 meters above Fairbanks in February 2021.

The mid-February period that exhibits strongest vertical differences in the two-height (20m and 3m) atmospheric composition measurements is highlighted in Figure 1b (where lightly shading denotes darkness, unshaded is sunlit). Surface NO and CO become enhanced in the evening just after dusk, reaching 2 ppmv and 100-200 ppbv, respectively at CTC base. There is also a smaller peak in these pollutants in the mid-morning. The maxima in these pollutants, CO and NO, are significantly lower on CTC roof, by approximately a factor of two or more. The measured NO₂ exhibits these same early-evening and mid-morning maxima, but NO₂ abundance is more similar at all sites, sometimes just slightly (~10 ppbv) lower at the roof at night. The range in NO₂ is between 20 to 50 ppbv, and the trend at all sites is typically decreasing during the night (after the evening NO_x peak) and increasing in the morning. Ozone exhibits an opposing and complementary trend to NO_x (NO+NO₂). During night, ozone becomes enhanced at CTC roof at 10-15 ppbv whilst it is low and near-zero at the surface. During the day (late morning) surface ozone increases. By mid-afternoon ozone reaches a uniform vertical distribution at 5-10 ppbv at all sites, marking the diurnal maximum surface abundance and only a local rooftop maximum. These diurnal patterns and vertical gradients in CO, NO_x and ozone can be readily qualitatively interpreted as the combined effects of local emissions (with early-evening and mid-morning maxima), pollution trapping by thermal inversions which develop during the night and inhibit vertical mixing, disruption of the inversions by solar heating during the day leading to strong vertical mixing, and atmospheric chemistry which interconverts NO, NO₂ and O₃.

The following sections discuss these aspects and present their characterisation or quantification through further analysis of the low-cost electrochemical sensor measurements over the whole 7 February – 9 March two height field-campaign period.

Low-cost sensing of O₃-NO-NO₂ atmospheric chemistry

Atmospheric chemistry exerts a strong control on the O₃-NO-NO₂ ppbv mixing ratios that is accurately captured by the electrochemical sensors: Ozone and NO₂ show an inverse relationship across the instrument time-series, Figure 1a,b. Reactions R1-R3 interconvert NO and NO₂ on minutes timescales under sunlit conditions.



The dynamic relation between observed NO, NO₂ and ozone is illustrated in Figure 2 (dimly daylight, and dark hours) for the measurements at NCORE, CTC base and CTC roof during February 7th to March 9th. The sensors and AQ monitors show

similar results, which reflects good instrument functioning (notwithstanding uncertainties in the span of the air quality monitor for ozone, see Methods). When NO_x exceeds ~50 ppbv, ozone is depleted and NO and NO₂ are enhanced. Despite the dimly-lit Fairbanks winter conditions, a dynamic equilibrium between NO, NO₂ and ozone can readily establish during sunlit daytime. The solar noon lifetime for NO₂ at Fairbanks latitude and longitude on 21 February is 6.1 minutes (Tropospheric Ultra-Violet and Visible Radiation Model v5.3^[30]), even without considering effects of enhanced albedo due to surface snow. During night, suppression of NO₂ photolysis leads to slightly higher NO₂ and lower NO and ozone compared to day, Figure 2.

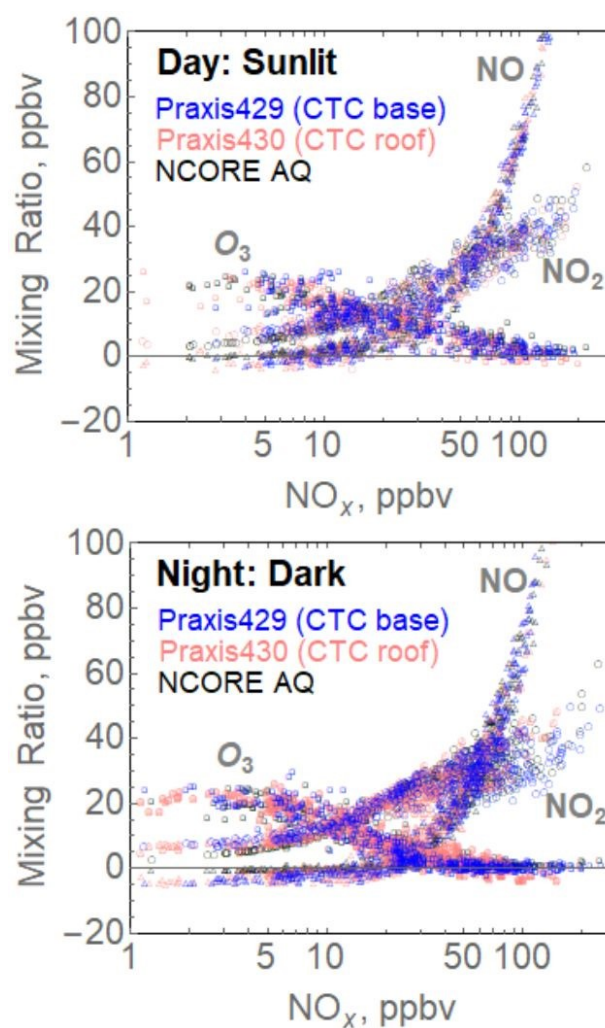


Figure 2. Low cost electrochemical sensing of the atmospheric chemistry relationship between NO, NO₂ and O₃ to NO_x (NO + NO₂) as measured during day and night during the field-campaign (7 February – 9 March 2021) in downtown Fairbanks. Sensors were located at 20m height on CTC roof (P430 sensor set, pink) and at 3m on CTC base (P429 sensor set, blue). To validate the ppbv-level low-cost electrochemical sensor measurements, a comparison is made to NO, NO₂ NO_x and O₃ measured by air quality monitors at the Fairbanks NCORE site (black), 500 m north of CTC site. Note log-scale for x-axis.



Thermal inversions, vertical mixing and emissions trapping

Temperature differences between surface and aloft

Near-surface inversions can be quantified from hourly temperature, differences between the surface (3m) and aloft, using the mast-based aspirated thermocouple temperatures, T , at 3m and 11m. We also calculate the difference in measured temperature of the electrochemical sensors, T_{sens} , at 3m and 20m, but that are subject to heating from their local instrument-environment, estimated at around 5 °C above ambient temperature based on comparing the 3m CTC base and 3m mast temperatures ($T_{\text{sens}}-T$), Figure 3 upper. Analysis of vertical gradients in temperature (T 11m-3m and T_{sens} 20m-3m divided by the vertical distances of 8m or 17m, respectively) finds a strong diurnal variation, Figure 3 lower. Both T and T_{sens} methods observe strongly stably stratified conditions during night, with average temperature gradients above +0.05 °C/m (i.e. nearly 1 °C between surface and rooftop developing on average each night). During daytime this positive gradient declines to unstable/neutral conditions, reflecting warming of the near-surface air through solar heating of the surface. Local solar noon is around 13h to 14h in Fairbanks, with peak surface temperature around 15h. The diurnal cycle derived from T_{sens} is somewhat skewed compared to the cycle from the mast T , and the T_{sens} daytime minimum substantially overshoots the adiabatic lapse rate (-0.0098 °C/m), likely reflecting slight differences in heating of the two instruments and their gas sensors during daytime surface warming. The 20m-3m T_{sens} -derived and 11m-3m T (mast) derived temperature gradients are nevertheless in quantitative agreement during night. In the following we used mast (11m-3m) T differences and a scaling factor $(20-3)/(11-3) = 17/8$ to estimate temperature differences between CTC roof and surface, for comparison to the measured vertical differences in pollutants between roof and surface.

Pollutant trapping < 20m by near-surface thermal inversions

A histogram approach is used to present differences in roof and surface pollution abundances, Figure 4. Data is categorised according to mast-based 11-3m temperature differences above and below a threshold of 0.5 °C, that was proposed by Cesler-Maloney et al.^[13] as an indicator of strong inversions causing near-surface pollution trapping during the 2019-2020 winter. The 7 February - 9 March 2021 dataset supports this choice of threshold: vertical differences in CO, NO, NO₂ and O₃ are close to zero (just slightly enhanced at surface by few ppbv) for $T_{11\text{m}-3\text{m}} \leq 0.5^\circ\text{C}$, whereas for $T_{11\text{m}-3\text{m}} > 0.5^\circ\text{C}$ the vertical differences are strongly skewed due to the near-surface trapping of pollutants by inversions, resulting in enhanced surface abundances of CO, NO, NO₂, and lower surface abundances of O₃ compared to at 20 m. The NO₂ distribution shows a more subtle pattern than CO or NO, as it also reflects the compensating role of atmospheric chemistry in converting NO into NO₂ where ozone is available, therefore exhibits a surface enhancement but is more evenly distributed between surface and rooftop.

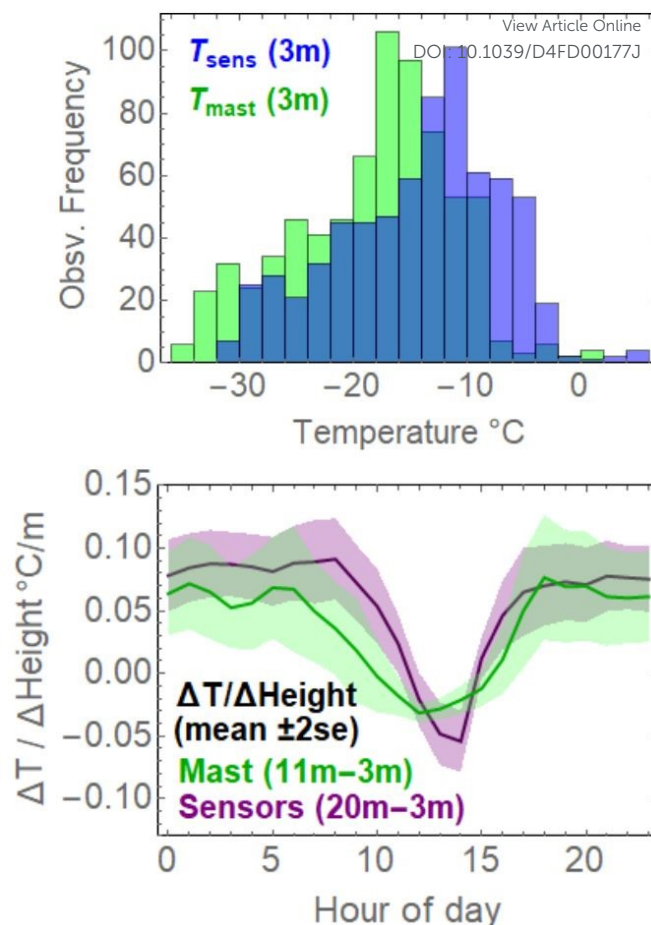


Figure 3. Upper: Histogram of hourly temperature measured at 3m on the mast (T , lighter gray) and the sensor temperature in Praxis P429 (T_{sens} , darker gray) showing consistent $\sim 5^\circ\text{C}$ instrument warming of T_{sens} compared to ambient T as measured on the mast during the field campaign. Lower: Diurnal cycle in hourly temperature gradient (temperature difference divided by height difference) measured using aspirated thermocouples over 11-3m on the mast (blue) and by the Praxis instrument gas sensor temperatures over 20-3m from CTC roof to surface (red), indicating the two methods show consistent trends and measured magnitudes of the night-time inversions, with some additional instrument-heating effects on gas sensor temperature during day.



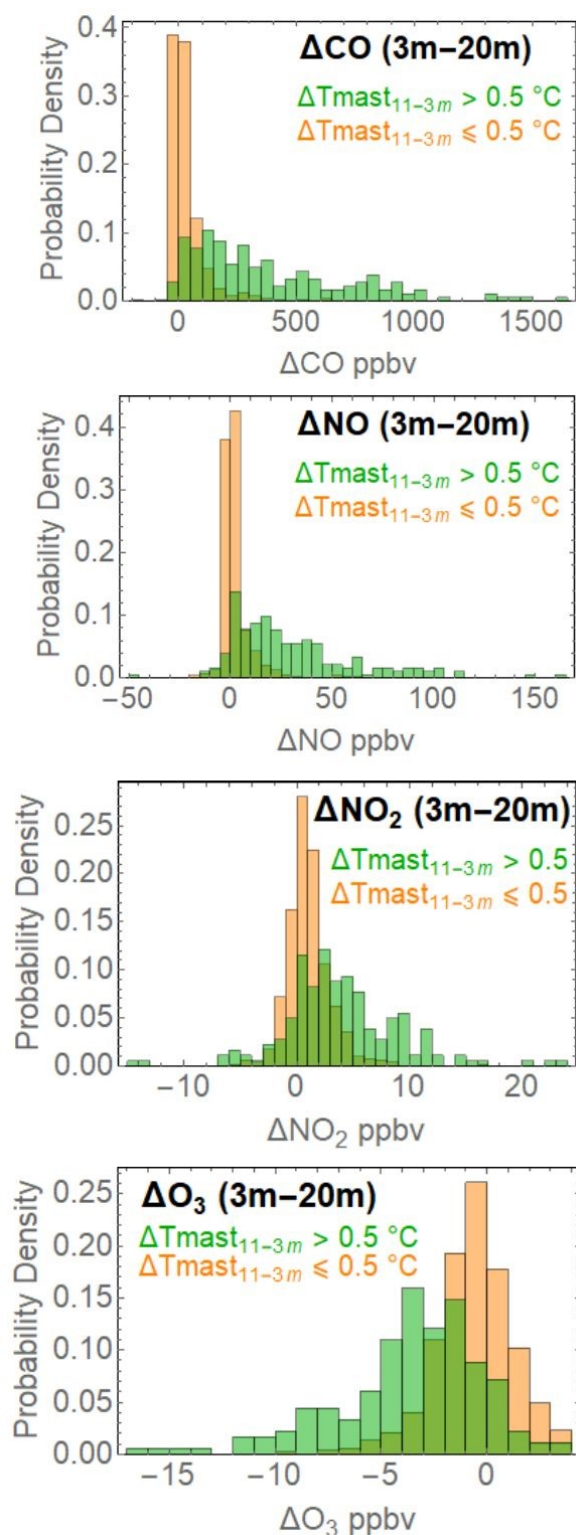


Figure 4. Probability histograms of the vertical difference (3m-20m) in hourly gas abundances measured between CTC surface and roof during the 7 February-9 March 2021 downtown Fairbanks field-campaign. Data is categorised above and below a 0.5°C threshold for the vertical 11m – 3m temperature differences co-measured on the nearby mast, as a measure of presence of absence of strong inversions, following Cesler-Maloney et al. [13].

The relationship between the roof-to-surface temperature difference (using 11m-3m mast data scaled to represent 20m-3m roof-surface differences, see above) and the roof-to-surface pollution difference is further quantified through scatter plots: Figure 5 shows the hourly vertical differences in pollutants versus hourly vertical differences in temperature for CO, NO, NO₂, O₃ and also NO_x (NO+NO₂) and O_x (NO₂+O₃). The near-surface locally emitted pollutants CO, NO and NO_x exhibit strong positive correlations between enhanced surface abundance (relative to rooftop) and greater temperature stability. At the most stable conditions (higher temperature difference between roof and surface), the magnitude in the vertical difference in these pollutants is most variable: very large differences may reflect periods with high emission fluxes under prolonged strongly stable conditions, leading to substantial CO, NO or NO_x pollutant accumulation at the surface. NO₂ and O₃ exhibit opposing trends that are generally more linear, reflecting their interconversion by atmospheric chemistry. The calculated linear regressions on vertical rooftop-to-surface differences in NO₂ and O₃ with vertical difference in temperature are approximately equal at +/- 0.8 ppbv per °C (calculated over 20m-3m). The corresponding trend in O_x (NO₂+O₃) is approximately flat, with vertical O_x difference around zero. This is expected given the near equal and opposite gradients in NO₂ and O₃. Processes that can form/destroy O_x or emission sources of O_x were comparatively small or more subtle during the field-campaign period, and are investigated through a diurnal data analysis below.

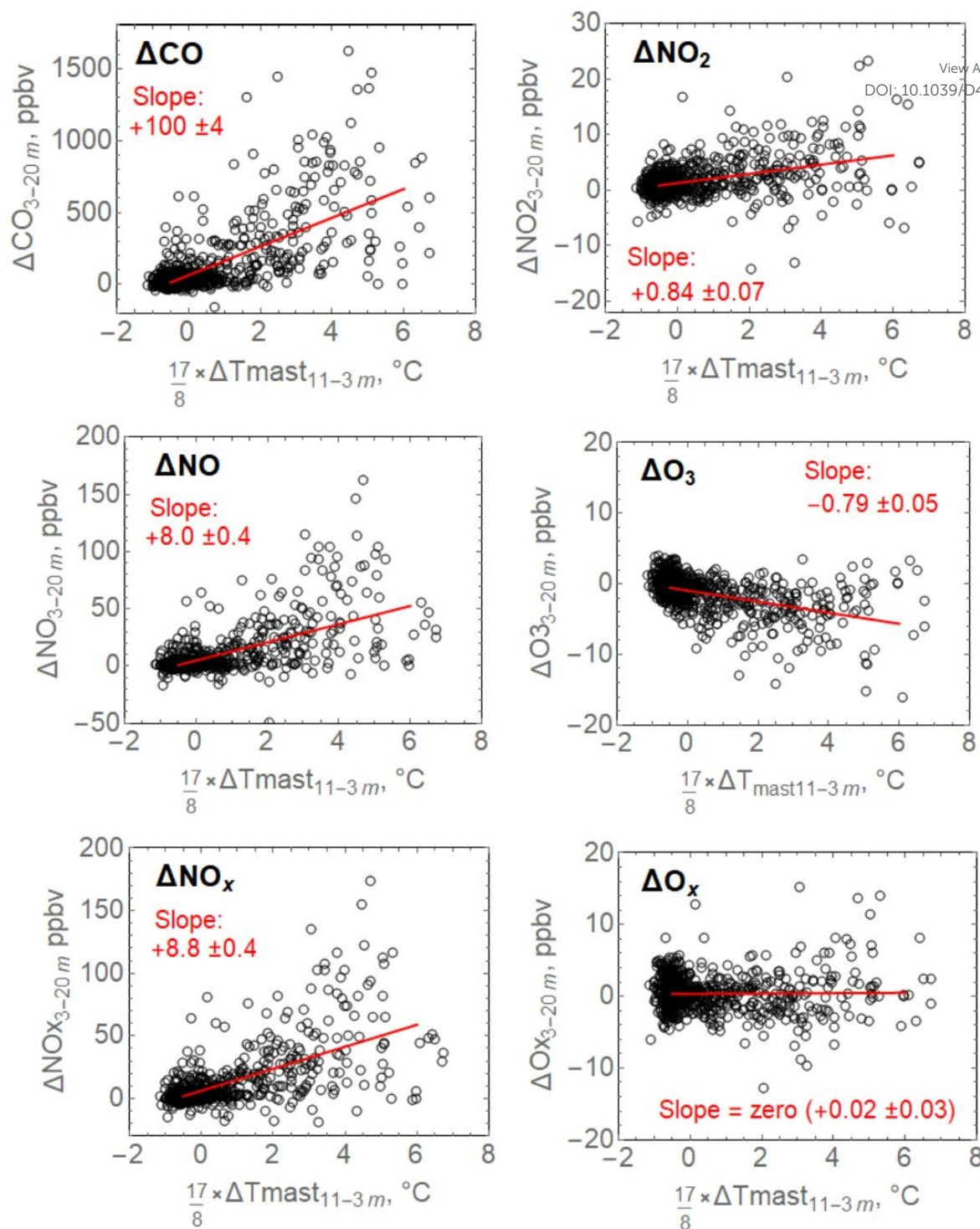


Figure 5. Scatter plots of vertical differences in gas abundance (at height: 3m – 20m) versus vertical difference in temperature (mast 11m-3m scaled by $(20-3)/(11-3) = 17/8$, to be equivalent to temperature difference over 20m-3m height). Note that this specific choice of axes gives positive trends for a greater near-surface trapping of pollutants (y-axis) with stronger thermal inversion (x-axis). Left-hand-column plots show positive (non-linear) trends for CO, NO and NO_x . Right-hand column plots show positive linear trend for NO_2 , negative linear trend for O_3 and no trend for O_x . Linear fits are presented for NO, O_3 , O_x , with slopes quantified.



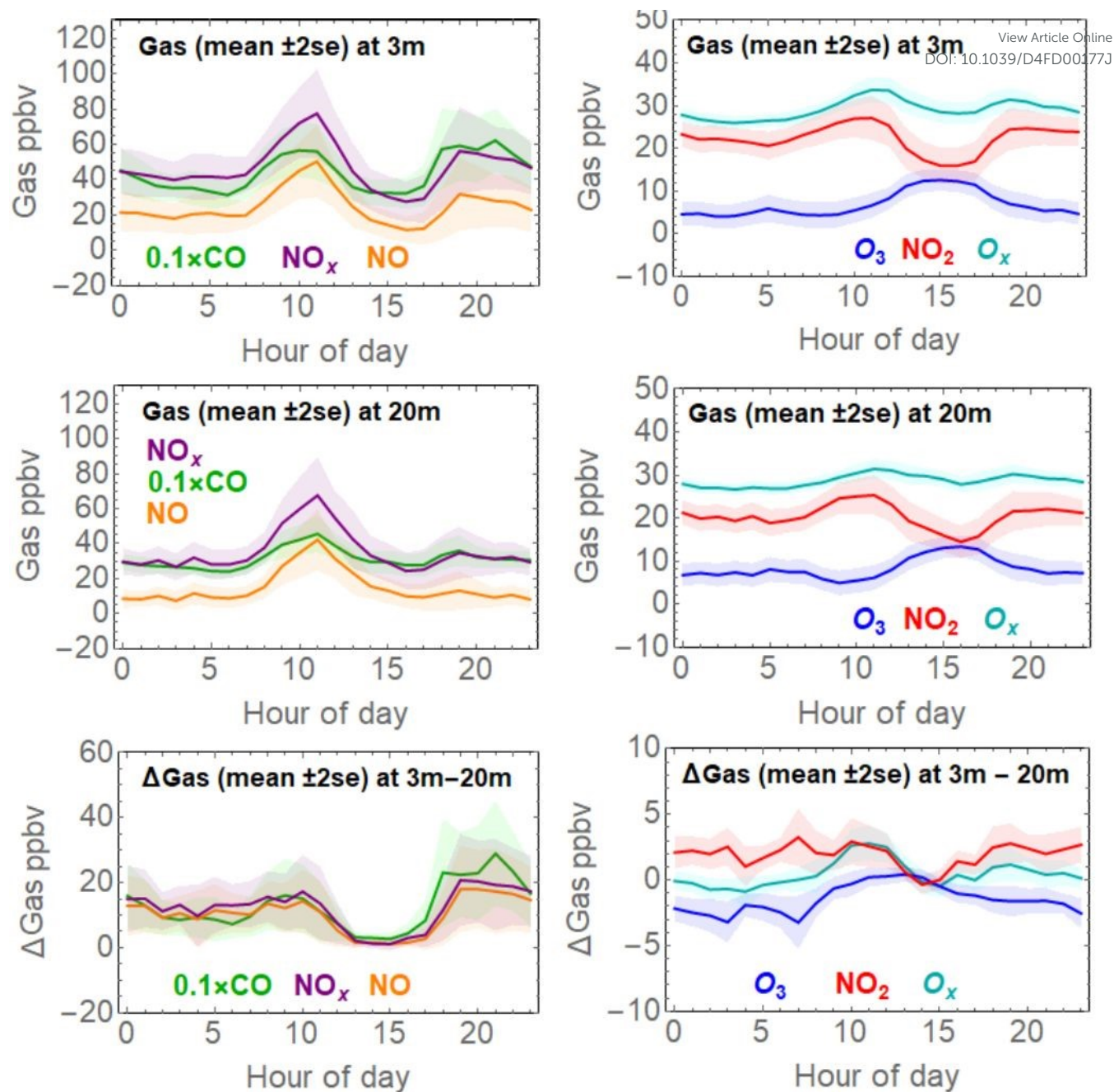


Figure 6. Diurnal variation in the hourly mean (line) ± 2 standard error (shaded region) gas composition measured by low-cost electrochemical sensors at CTC base (3m), CTC roof (20m) and vertical difference (3m-20m) during the 7 February – 9 March 2021 field-campaign in downtown Fairbanks. Left-hand column shows $CO/10$ (green), NO_x (purple) and NO (orange). Right-hand column shows NO_2 (red), O_3 (dark blue) and O_x (light blue). Hour is local hour from 0 to 23.



Diurnal changes in atmospheric composition at the surface and 20m above Fairbanks.

Diurnal trends in the surface (3m) and rooftop (20m) abundances of CO, NO, NO_x and NO₂, O₃ and O_x as well as their vertical differences (3m-20m) is shown through their hourly mean and standard error during the field-campaign (7 February to 9 March 2021), Figure 6. As a data quality check, differences between these sensors are also calculated for the 9 March – 31 March period when they were co-located at 3m at NCORE, confirming that potential diurnal biases are very small (few ppbv), Supplementary Material Figure S3. The diurnal temperature gradient during the 7 February to 9 March 2021 field-campaign, Figure 4(lower), quantified the inversions with strongly stable conditions that enhance pollutant trapping during night, but are disrupted during daytime to enable efficient vertical mixing during the afternoon. Another factor controlling the diurnal pollutant abundances, their trends and vertical differences is the diurnal variation in local emissions. Inspection of Figure 6 can enable to qualitatively detangle these two convoluted effects and identify key controls on Fairbanks surface and near-surface atmospheric composition. Hourly mean CO, NO, NO_x surface pollution exhibits twice daily maxima in the mid-morning (10-11 am) and early evening (7-8 pm), with a daily minimum around 3 pm, and similar variations are seen for NO₂ over much smaller ppbv scale. Conversely, for the rooftop data only the morning pollution maximum is clearly evident. The vertical differences confirm that efficient trapping of early evening emissions below 20m is responsible for surface night-time pollution whereas the morning emissions yield similar surface abundances but mix up to higher heights to (above) 20m. This suggests a particularly strong mid-morning emission flux that is also more NO_x-rich than in the evening. Ozone shows the inverse behaviour to NO₂ with lower ozone at the surface (~5 ppbv) than aloft (~10 ppbv). This is due to ozone titration by reaction with NO that occurs at both levels but to a greater extent at the surface where NO_x is most abundant. The measured vertical difference in ozone is eroded during the morning concurrent with NO_x emissions partially mixing up to 20m. Subsequently, in the mid-afternoon ozone becomes enhanced at both the surface and at 20m to around 15 ppbv at 3-4pm. This indicates an efficient vertical mixing that brings down ozone-rich air from further aloft. Concurrently, both the surface and rooftop pollutant abundances diminish. The atmosphere is measured to be vertically uniform in CO, NO, NO₂, O₃ composition between 3 and 20m at around 14-15h. Pollutant abundances then increase (and ozone decreases) as the sun sets and thermal inversions can develop again to trap the local emissions. O_x abundances are broadly similar at the rooftop and surface as previously noted, but the diurnal trend in O_x is not flat. At the surface (and to a lesser extent on the rooftop) O_x is enhanced during the morning and evening emission peaks, particularly in the mid-morning when NO_x is most enhanced, also highlighted by the vertical difference in O_x. This suggests a local emission source of O_x as well as NO_x that is further characterised and quantified below. It has also been hypothesized that O_x loss processes may occur in the

atmosphere above Fairbanks during night, via NO₃-N₂O₅ chemistry to form nitrate under moderately polluted and dark conditions when ozone and NO₂ are present.^[13] Such processes are difficult to elucidate using this hourly-averaged two-height dataset but are being investigated with higher time resolution data, including ALPACA 2022 Fairbanks campaign measurements by low-cost electrochemical sensor.

Characterising Fairbanks emissions using low-cost sensors

Fairbanks NO_x emissions. NO_x exerts a key role in atmospheric chemistry and NO₂ is an important regularised component in air quality monitoring. However, unlike for CO and particles, NO_x emissions data is limited for Fairbanks, and may be underestimated^[31]. NO_x emissions are evident in Figure 6 during both morning and evening. Comparison of the CO and NO_x (NO+NO₂) ratios measured at NCORE, CTC base and roof enables to characterise the local NO_x emissions, Figure 7. Linear regressions find the measured CO/NO_x ratios (5.2 to 5.8 ±0.1 mol/mol, equivalent to 0.18±0.01 mol/mol NO_x/CO) are in good agreement between all instruments when located at NCORE (i.e. sensor algorithm fitting period in January and March). When the sensors were located at CTC roof and base during February the measured CO/NO_x ratios are also broadly similar, at 4.6 to 7.3 (±0.1) mol/mol (equivalent to a NO_x/CO ratio of 0.14 to 0.22 mol/mol). The CO versus NO_x data clouds from the low-cost sensors and NCORE analysers strongly overlap at moderate pollution levels (<100 ppbv NO_x or 500 ppbv CO). Spread in CO/NO_x is more evident for the few observations at higher pollution levels. This likely reflects a combination of variations in local emissions (e.g. traffic, home-heating) over time and location as a function of source mixes and temperatures (e.g. as seen in Figure 6 diurnal means) as well as instrument uncertainties. Higher CO/NO_x at CTC base may be expected as it is geographically more exposed to CO-rich road traffic emissions. CTC is also surrounded by a slightly greater density of homes. Finally, we note the regression lines in Figure 7 yield intercepts (95-180 ppbv) consistent with CO tropospheric background.



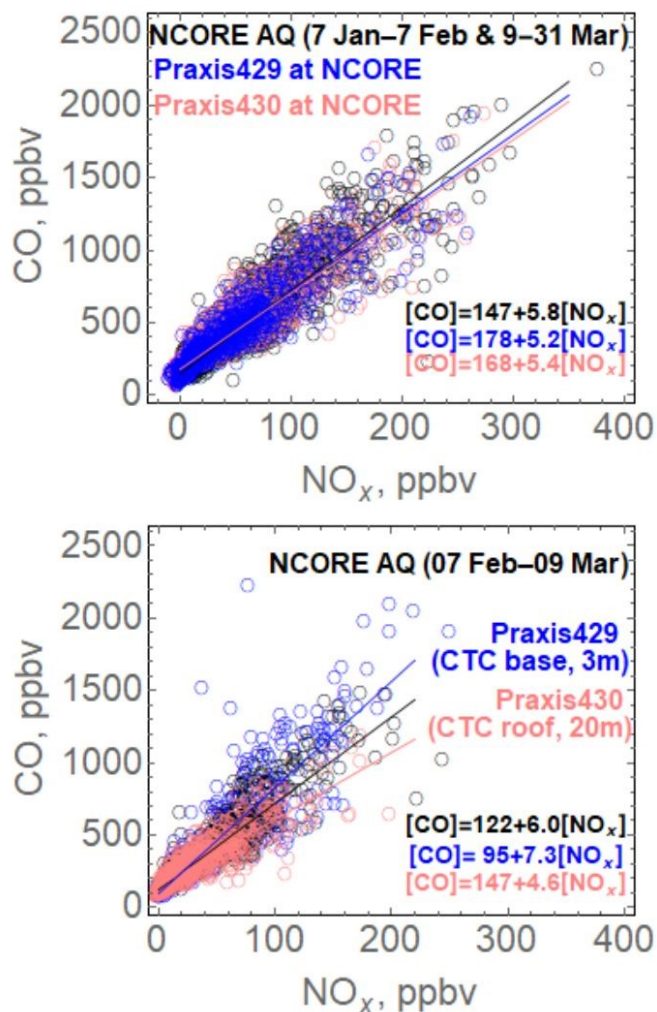


Figure 7. Scatter plot of hourly CO (ppbv) versus NO_x (NO+NO₂, ppbv) measured by low-cost electrochemical sensors in Fairbanks, at the NCORE site (7 Jan – 7 Feb and 9 Mar – 31 Mar 2021, P430 in pink and P429 in blue), and at the CTC site (7 Feb–9 Mar, P430 at 20m on rooftop in pink, P429 at 3m at CTC base in blue), upper and lower plots respectively. Shown alongside are hourly data from Air quality analysers at NCORE for the same periods (black). Linear-regressions are calculated for each dataset, with gradient quantifying the CO:NO_x ratio under polluted conditions at each location and intercept providing an estimate of background CO mixing ratio at low NO_x conditions.

A source of O_x in Fairbanks. During the 2021 winter, O_x co-varied by 10's of ppbv at NCORE, CTC base and CTC roof (Figure 8). In all periods and sites, maxima in O_x (NO₂+O₃) tend to be accompanied by high NO_x (NO+NO₂), e.g. Figure 1b, Figure 6. As reactions R1-3 conserve O_x (the sum of NO₂ and Ozone), other processes must be responsible for the observed variations in O_x. Sources of O_x are particularly pertinent during the darkest Fairbanks winter months when slow photolysis limits the formation of oxidants, and ozone is typically titrated by high NO emissions. The correlation between O_x (as NO₂) and NO_x

identified by low-cost sensors is confirmed by analysis of NCORE air quality monitoring datasets over seven Fairbanks winter seasons (November to February, 2015–2016 to 2020–2021), Figure 8. The multi-year average O_x:NO_x ratio is 0.13 mol/mol (calculated on all data where NO_x > 50 at NCORE, with range 0.12–0.15 mol/mol for the individual winters, except 0.06 mol/mol in 2019–2020). The NO_x-dependent source of O_x is observed across all dimly-lit and dark Fairbanks winter months, thus likely reflects a 'primary' or 'direct' emission of NO₂, rather than a photochemical origin. A possible emission source is vehicular primary emissions of NO₂. Our observed NO₂/NO_x of 0.13 mol/mol in Fairbanks is within the range reported by studies of European road traffic^[32] but is more than double the ratio of 0.053 mol/mol found in a study of US road traffic in Denver Colorado^[33]. The high NO₂/NO_x is somewhat surprising: vehicular traffic is typically gasoline-dominated in the United-States in contrast to Europe where diesel fuel is largely responsible for high NO₂ emissions. Alaskan cities such as Fairbanks may have a higher proportion of diesel vehicles than cities in other US states. Also, vehicular emissions of oxidised nitrogen species such as NO₂, HONO can be enhanced under 'cold-start'/cold driving conditions below 5°C, a phenomenon that occurs for all fuel-types^[34]. Further investigation of the source(s) of the 'primary' or 'direct' NO₂ emissions in Fairbanks is warranted in the context of the recently strengthened WHO air quality guidelines^[35] for NO₂ and to understand the impact of sources of oxidised reactive nitrogen on Fairbanks wintertime atmospheric chemistry.



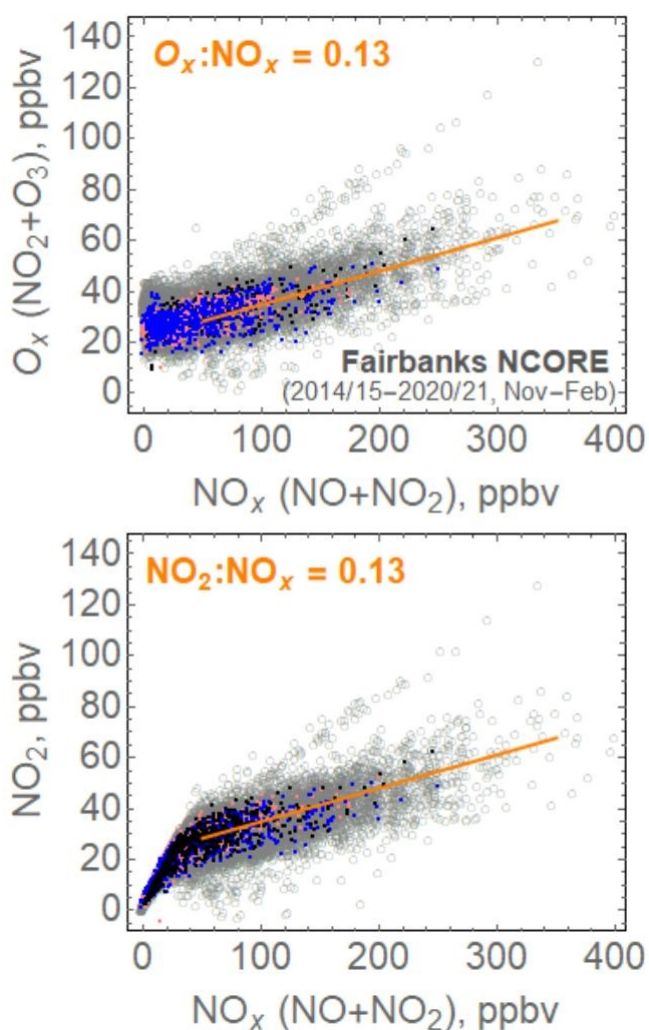


Figure 8. Hourly O_x (O_3+NO_2) versus NO_x ($NO + NO_2$) and NO_2 versus NO_x measured by electrochemical sensor during the field-campaign (P430 in pink, P429 in blue, measured at CTC roof and base, respectively, see caption of Figure 7), and measured by Air quality Monitors at NCORE during the field-campaign (black) and during the six preceding winters November-February from 2014-15 up to 2020-21 (gray open circles). The average $O_x:NO_x$ and $NO_2:NO_x$ emission ratios are calculated using NCORE data with $NO_x > 50$ ppbv.

Conclusions

This study demonstrates low-cost electrochemical sensing of CO , NO , NO_2 and O_3 under cold and wide-ranging temperatures ($0^\circ C$ down to $-30^\circ C$). We show that low-cost electrochemical gas sensors can deliver quantitative characterisation of atmospheric composition at the ppbv-level, that is sufficiently robust to investigate atmospheric chemistry. We demonstrate that autonomous instruments containing low-cost electrochemical sensors can provide continuous quantitative monitoring of Arctic atmospheric composition over weeks-to-

month timescales, even under harsh Arctic conditions. Sensor deployments in downtown Fairbanks in February-March 2021 quantify $CO:NO_x$ compositions of local emissions and provide evidence for primary emissions of NO_2 that could be an important O_x oxidant source under the low ozone conditions of downtown Fairbanks in winter. Sensor deployments at two heights characterise the vertical distribution in air composition. Surface trapping of locally emitted pollutants at night occurs over very short vertical scales that can be less than 20m during strong temperature inversions. This leads to short-scale vertical gradients in oxidants relevant to atmospheric chemistry: surface ozone is depleted by NO_x whilst ozone can be present at 20m aloft. The inversions observed during February-March 2021 are short-lived as they are disrupted by efficient vertical mixing during daytime due to solar heating. During the predominantly dark mid-winter, inversions and pollutant trapping can be longer-lived, leading to multi-day episodes of severe air quality. Local mediation efforts seek to further mitigate against poor air quality through reducing local emissions, building on achieved improvements in e.g. CO exceedances compared to previous decades^[4-6]. However, the accumulation of pollutants at the surface is difficult to prevent when vertical mixing is limited by the development of stable temperature gradients and the Fairbanks basin that is shielded by surrounding hills. The observed very short vertical scale of pollutant trapping with cleaner air just a few tens of meters aloft might offer potential for future geoengineering solutions to contribute to improving Fairbanks indoor or outdoor air quality during severe surface pollution events, for example via introducing mechanical vertical mixing or by smart buildings with routing of clean air streams down from aloft, supported by automated real-time monitoring. This study presents low-cost electrochemical gas sensors as a valuable tool to measure atmospheric composition in the polluted Arctic at ppbv-level suitable for emissions characterisation and for tracing atmospheric chemistry and fine-scale differences with height. The methods can also be applicable to the study of other urban wintertime environments where local emissions, temperature inversions and limited vertical mixing can lead to accumulation of pollutants at the surface and degraded air quality.

Author contributions

All authors (T. J. Roberts, M. Cesler-Maloney, W. R. Simpson): Conceptualization, Methodology, Software, Validation, Formal analysis, Investigation, Resources, Data curation, Writing - original draft, Writing - review & editing, Visualization, Project administration, Funding acquisition

Conflicts of interest

There are no conflicts to declare.

Data availability



Data for this article, including air quality monitor and sensor gas measurements and mast-based temperature measurements are available at OSF at <https://doi.org/10.17605/OSF.IO/UMDGW>.

Acknowledgements

This research analysis was undertaken through the ENS-PSL University Actions Incitatives sENSE project and ANR consortium project VOLC-HAL-CLIM, with small grant co-funding from Observatoire de Versailles Saint-Quentin-en Yvelines (OVSQ). It contributes essential sensor preparations for mobile vertical profiling applications planned in ANR CASPA, and for rooftop monitoring undertaken in ALPACA 2022.

References

- J. Schmale, J., S. R. Arnold, K. S. Law, T. Thorp, S. Anenberg, W. R. Simpson...K. A. Pratt. *Earth's Future*, 2018, **6(10)**, 1385-1412. doi:10.1029/2018ef000952
- T. Ward, B. Trost, J. Conner, J. Flanagan, R. K. M. Jayanty. *Aerosol and Air Quality Research*, 2012, **12(4)**, 536-543. doi:10.4209/aaqr.2011.11.0208
- Y. Wang, P. K. Hopke. *Aerosol and Air Quality Research*, 2014, **14(7)**, 1875-1882. doi:10.4209/aaqr.2014.03.0047
- J. Holty. *Arctic*, 1973, Dec., **26**, No. 4 (Dec., 1973), pp. 292-302
- T. M. Gilmore, and T. R. Hanna, *Journal of the Air Pollution Control Association*, 1974, **24**, 11, 1077-1079.
- S. A. Bowling, *Journal of Climate and Applied Meteorology*, 1985, **25**, pp22-34
- H. N. Q. Tran, & N. Mölders, *Atmospheric Research*, 2011 **99(1)**, 39-49. doi:10.1016/j.atmosres.2010.08.028
- C. D. Whiteman, C. D., S. W. Hoch, J. D. Horel, and A. Charland, *Atmos. Environ.*, 2014, **94**, 742-753, <https://doi.org/10.1016/j.atmosenv.2014.06.012>.
- Y. Largeron Y. and S. Staquet, *Atmospheric Environment*, 2016, **135**, 92-108, <https://doi.org/10.1016/j.atmosenv.2016.03.045>
- A. G. Hallar, S. S. Brown, E. Crosman, et al., *Bulletin of the American Meteorological Society*, 2021, **102**, 10, E2012-E2033, <https://doi.org/10.1175/BAMS-D-20-0017.1>
- S. M. Bourne, U. S. Bhatt, J. Zhang, J., R. Thoman. *Atmospheric Research*, 2010, **95(2-3)**, 353-366. doi:10.1016/j.atmosres.2009.09.013
- J. A. Mayfield, G. J. Fochesatto. *Journal of Applied Meteorology and Climatology*, 2013, **52(4)**, 953-973. doi:10.1175/jamc-d-12-01.1
- M. Cesler-Maloney, W. R. Simpson, T. Miles, J. Mao, K. S. Law T. J. Roberts, *JGR Atmospheres*, 2022, **127**, 10, <https://doi.org/10.1029/2021JD036215>
- E. S. Robinson, M. Cesler-Maloney, X. Tan, J. Mao, W. R. Simpson, P. F. Decarlo, *Environmental Science: Atmospheres*, 2023, DOI: 10.1039/d2ea00140c
- M. I. Mead, O. A. M. Popoola, G. B. Stewart, P. Landshoff, M. Calleja, M. Hayes, J. J. Baldovi, M. W. McLeod, T. F. Hodgson, J. Dicks, A. Lewis, J. Cohen, R. Baron, J. R. Saffell, R. L. Jones, *Atmos. Environ.*, 2013, **70**, 186-203.
- I. Heimann, V. B. Bright, M. C. McLeod, M. I. Mead, O. A. M. Popoola, G. B. Stewart, R. L. Jones, *Atmospheric Environment*, 2015, **113**, 10-19, <https://doi.org/10.1016/j.atmosenv.2015.04.057>
- W. Jiao, G. Hagler, R. Williams, R. Sharpe, R. Brown, D. Garver, R. Judge, M. Caudill, J. Rickard, M. Davis, U. Weinstock, J. S. Zimmer-Dauphinee, K. Buckley., *Atmos. Meas. Tech.*, 2016, **9**, 5281-5292, <https://doi.org/10.5194/amt-9-5281-2016>.
- A. C. Lewis, J. D., Lee, P. M. Edwards, M. D. Shaw, M. J. Evans, S. J. Moller, K. R. Smith, J. A. Buckley, M. Ellis, S. R. Gillot, A. White.. *Faraday discussions*, 2016, **189**, 85-103.
- N. Castell, F. R. Dauge, P. Schneider, M. Vogt, U. Lerner, B. Fishbain, D. Broday, A. Bartonova., *Environ. Int.*, 2017, **99**, 293-302, <https://doi.org/10.1016/j.envint.2016.12.007>.
- E. S. Cross, L. R. Williams, D. K. Lewis, G. R. Magoon, T. B. Onasch, M. L. Kaminsky, D. R. Worsnop, J. T. Jayne, *Atmos. Meas. Tech.*, 2017, **10**, 3575-3588, <https://doi.org/10.5194/amt-10-3575-2017>.
- X. Pang, X., M. D. Shaw, A. C. Lewis, L. J. Carpenter, T. Batchellier T., , 2017, *Sensors and Actuators B: Chemical*, **240**, 829-837, <https://doi.org/10.1016/j.snb.2016.09.020>.
- N. Zimmerman N., A. A. Presto, P. N. S. Kuma, J. Gu, A. Haruyliuk, E. S. Robinson, A. L. Robinson, R. Subramanian, *Atmos. Meas. Tech.*, 2018, **11**, 291-313, <https://doi.org/10.5194/amt-11-291-2018>, 2018.
- R. Baron and J. Saffell (2017), *ACS Sens.*, 2017, **2**, 11, 1553-1566, <https://doi.org/10.1021/acssensors.7b00620>
- D. E. William, *ACS Sensors*, 2019, 2258-2656, doi: 10.1021/acssensors.9b01455
- B. Crawford, D. H. Hagan, I. Grossman, E. Cole, L. Holland, C. L. Heald, and J. H. Kroll, *PNAS*, 2021, **118** (27), e2025540118. doi:10.1073/pnas.2025540118.
- T. Bush, N. Papaioannou, F. Leach, F. D. Pope, A. Singh, G. N. Thomas, B. Stacey, S. Bartington S., *Atmos. Meas. Tech.*, 2022 **15**, 3261-3278, <https://doi.org/10.5194/amt-15-3261-2022>
- R. Whitty, M. Pfeffer, E. Ilyinskaya, T. Roberts, A. Schmidt, S. Barsotti, W. Strauch, L. Crilley, F. Pope, H. Bellanger, E. Mendoza, T. Mather, E. Liu, N. Peters, I. Taylor, H. Francis, X. Hernández Leiva, . Lynch, S. Nobert, P. Baxter. *Volcanica*, 2022, **5(1)**, pp. 33-59. doi: 10.30909/vol.05.01.3359.
- T.J. Roberts, C.F. Braban, C. Oppenheiler, R. S. Martin, R. A. Freshwater, D. H. Dawson, P. T. Griffiths, R. A. Cox, J. R. Saffell, R. L. Jones, *Chemical Geology*, 2012, **332-333**, 74-91, <https://doi.org/10.1016/j.chemgeo.2012.08.027>
- M. Hossain M., J. R. Saffell, R. Baron R., *ACS Sensors*, 2016, **1**, 11, 1291-1294, DOI: 10.1021/acssensors.6b00603
- TUV model website : <https://www2.acom.ucar.edu/modeling/tropospheric-ultraviolet-and-visible-tuv-radiation-model>, https://www.acom.ucar.edu/Models/TUV/Interactive_TUV/
- N. Brett, K. S. Law, Steve R. Arnold et al. *ACPD preprint in review*, 2022, <https://doi.org/10.5194/egusphere-2024-1450>
- S. K. Grange, A. C. Lewis, S. J. Moller, D. C. Carslaw. *Nature Geosciences*, 2017, **10**, 914-918. <https://doi.org/10.1038/s41561-017-0009-0>
- R. J. Wild, W. P. Dubae, K. Aikin, S. J. Eilerman, A. Neuman, J. Peischl, T. B. Ryerson, S. S. Brown, *Atmospheric Environment*, 2017, **148**, 182- 189. doi: 10.1016/j.atmosenv.2016.10.039
- V. N. Matthaios, L. J. Kramer, R. Sommariva, F. D. Pope, W. J. Bloss, *Atmospheric Environment*, 2018, doi: <https://doi.org/10.1016/j.atmosenv.2018.11.031>.
- World Health Organization. 2021 WHO global air quality guidelines. <https://apps.who.int/iris/handle/10665/345334>. Licence: CC BY-NC-SA 3.0 IGO



Data availability

View Article Online
DOI: 10.1039/D4FD00177J

Data for this article, including air quality monitor and sensor gas measurements and mast-based temperature measurements are available at OSF at <https://doi.org/10.17605/OSF.IO/UMDGW>.

Open Access Article. Published on 24 January 2025. Downloaded on 2/21/2025 12:52:34 PM.
This article is licensed under a Creative Commons Attribution-NonCommercial 3.0 Unported Licence.

